ELSEVIER

Journal of Crystal Growth 159 (1996) 771–775

JOURNAL OF CRYSTAL GROWTH

$\chi^{(3)}$ Nonlinear susceptibility in II–VI compounds and applications for squeezed light generation in semiconductors

A.M. Fox, M. Dabbicco *, J.J. Baumberg [1], B. Huttner [2], J.F. Ryan

Department of Physics, University of Oxford, Clarendon Laboratory, Parks Road, Oxford OX1 3PU, UK

Abstract

We have measured the nonlinear refractive index near half-bandgap ($E_g/2$) in ZnS and ZnSe by self-phase modulation experiments. The ratio of the nonlinear phase shift and the total optical absorption losses is critically dependent on the detuning from $E_g/2$. Efficient quadrature squeezing was obtained at a centre wavelength of 780 nm in ZnS and at 960 nm in ZnSe. The scheme we employed can generally be applied to semiconductors, and opens the way for squeezed light generation over a wide range of wavelengths.

Squeezed states of the electromagnetic field are characterized by the presence of correlated pairs of photons. Hence, since the earliest days of squeezing theory, nonlinear optical systems which display two-photon processes have been indicated as most appropriate to generate these states. Semiconductors with a second-order $\chi^{(2)}$ nonlinear susceptibility are then the favoured candidates for quadrature squeezing [1] and for twin beam correlation [2]. The drawback of these materials is that it is only possible to generate squeezed light at a frequency different from that of the pump laser. On the other hand, third-order $\chi^{(3)}$ nonlinearities allow for frequency mixing and in particular *degenerate* frequency mixing so that squeezed light can be generated in the vicinity of the pump frequency. The drawback in this case is the much smaller efficiency of the process, which then requires higher laser power.

The compromise to obtain large and fast optical $\chi^{(3)}$ nonlinearities in semiconductors has always been critical. A generic figure of merit (M) for ultrafast non-resonant optical nonlinear applications is expressed by:

$$M = \frac{\Delta\phi_{\mathrm{NL}}}{\alpha L} \gg 1, \tag{1}$$

where $\Delta\phi_{NL}$ is the total nonlinear phase shift proportional to the nonlinear refractive index n_2, α is the optical absorption coefficient and L is the sample length. In a semiconductor, M is expected to be a strong function of energy relative to the bandgap E_g. Close to the bandedge n_2 is large but the absorption losses offset its effect to a great extent. For example, experiments on GaAs/GaAlAs waveguides found that two-photon absorption ultimately limited M to ~ 4 [3]. The other spectral region of interest is near $E_g/2$ where n_2 has a broad midgap resonance [4] and α is small (well below $E_g/2$ two-photon absorption is forbidden and higher order multi-photon

* Corresponding author. Fax: +44 1865 272400; E-mail: m.dabbicco@physics.ox.ac.uk.

[1] Present address: Hitachi Cambridge Laboratory, Madingley Road, Cambridge CB3 0HE, UK.

[2] Present address: NTT Basic Research Laboratories, 3-1 Morinosato Wakamiya, Atsugi, Kanagawa 243-01, Japan.

SSDI 0022-0248(95)00712-1

absorption processes are negligibly small except at the highest intensity), but n_2 also is considerably smaller. The spectral region of interest is therefore close to $E_g/2$. We demonstrate that M can be as large as 100 at energy below half-bandgap and that an appropriate choice of the energy detuning from $E_g/2$ is necessary to obtain large nonlinear effects.

We chose to work with wide bandgap semiconductors because of the half-bandgap energy lying at ~ 0.8 μm, which is of interest, for example, in short range communication systems. We studied ZnS and ZnSe samples in the form of 2 mm thick optical windows. The experiments were performed at room temperature using a Ti:sapphire laser with a tuning range 750–960 nm. In order to produce the required intensity, the laser was modelocked: the pulse train consisted of transform limited $\tau_p = 65$–125 fs pulses at 82 MHz repetition frequency, and the average power could be varied up to 1 W.

We first measured the nonlinear absorption and self-phase modulation as a function of the incident power. In Fig. 1 we present the transmitted spectra of self-phase modulated pulses for the case of ZnS. In order to fit the experimental results (dots), the pulse broadening has been modelled assuming a nonlinear phase shift proportional to the pulse intensity [5]

$$\Delta\phi(t) = (2\pi/\lambda) n_2 I(t) L_{\text{eff}}, \qquad (2)$$

where L_{eff} is an effective optical length defined by the confocal parameter

$$L_{\text{eff}} = 2 z_R \tan^{-1}(L/2 z_R),$$

and

$$z_R = \pi w_0^2 n_0/\lambda_0.$$

Here w_0 is the radius of the focusing spot at $1/e$ of the peak irradiance and λ_0 is the central wavelength. The intensity spectrum is then given by $I(\omega) \propto \|F(\omega)\|^2$ where $F(\omega)$ is the Fourier transform of the pulse amplitude

$$F(\omega) = (1/2\pi) \int E(t) e^{i\Delta\phi(t)} e^{-i(\omega-\omega_0)t}\, dt. \qquad (3)$$

The solid lines in Fig. 1 show the results of the fit using Eq. (3) and a symmetric $sech^2$ pulse profile, the pulse width being determined by the fit of the input pulses (dashed lines). The values of $\Delta\phi_{MAX}$ obtained by this procedure are reported in Fig. 2a.

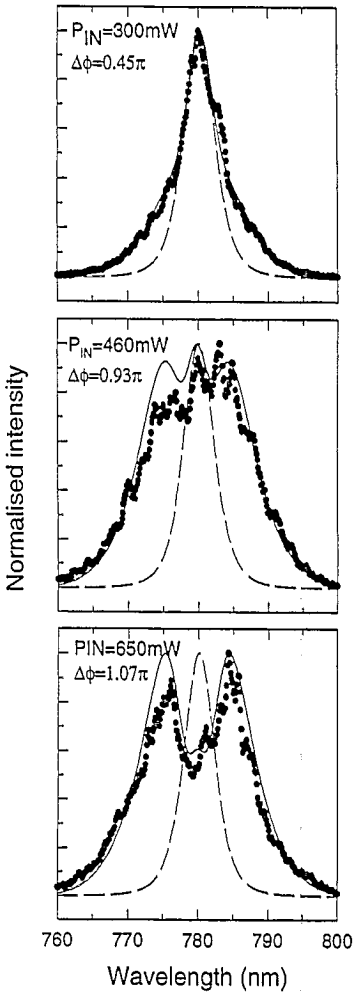

Fig. 1. Self-phase modulated spectra (dots) of the input pulses (dashed lines) through a 2 mm tick polycrystalline ZnS sample. The pulse width is 125 fs. The solid lines are the fit as described in the main text.

The linear regression fit through the data in Fig. 2a gives us $n_2 = (1.1 \pm 0.2) \times 10^{-14}$ cm^2/W at 780 nm, which is in good agreement with the value reported in Ref. [6] of 2.1×10^{-12} esu (0.7×10^{-14} cm^2/W) at the same wavelength, and also with theoretical predictions [4].

Fig. 2b shows the transmitted power as a function of input power. Up to ~ 300 mW (peak intensity ~ 14 GW/cm^2) the output is a linear function of input with a transmissivity close to unity, at higher input power nonlinear absorption processes start to cause saturation (two-photon absorption can be ruled

out because $\hbar\omega_0 \sim 0.43E_g^{ZnS}$ is far below the two-photon absorption edge). In the linear regime (below 300 mW) we estimate an upper value of the internal loss of the sample to be 1%, and thus obtain a value of $M > 100$.

In ZnSe at 960 nm ($\hbar\omega \sim 0.48E_g^{ZnSe}$) we measured a comparable value for M, whereas working close to $E_g/2$, at 934 nm, we obtained a larger nonlinear refractive index ($n_2 = (2.7 \pm 0.6) \times 10^{-14}$ cm^2/W) but the absorption losses due to two-photon absorption ($\beta = (0.3 \pm 0.05)$ cm/GW) limited the figure of merit to $M \sim 4$.

The large value of M obtained in both ZnS and ZnSe below $E_g/2$ allowed us to generate squeezed light fairly efficiently with a relatively straightforward experimental setup. Fig. 3 shows a schematic diagram of our squeezing apparatus (see Ref. [7] for details). The squeezed light is generated in the sidebands of the longitudinal laser modes by four-wave mixing after a single pass through the semiconductor. In order to separate the squeezed light from the laser modes a Sagnac interferometer is used [8,9]. In this configuration, the pump beam is incident on the input port of a 50:50 beamsplitter BS2, while vacuum noise enters through the other unused port. The two counter-propagating pump pulses are focused into the semiconductor sample to a spot of radius $w_0 = 8$ μm. The collimated transmitted beams recombine at BS2 where they interfere. The vacuum noise co-temporal with the pump pulses is squeezed in the semiconductor, and also recombines at BS2. In ideal conditions (perfect balancing of the interferometer) "bright" squeezed light is returned along the pump beam direction and the squeezed "vacuum" emerges at the unused port.

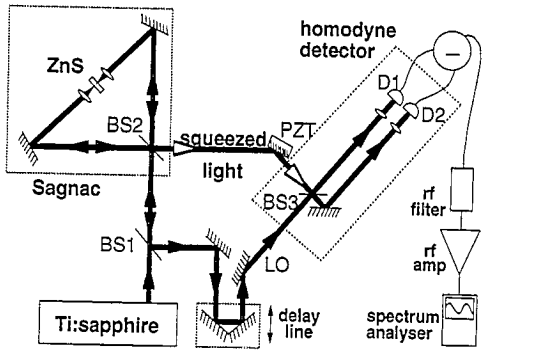

Fig. 3. Schematic diagram of the apparatus used to generate the squeezed light. BS1 is a 15:85 beam splitter; BS2 and BS3 are 50:50 beam splitters. The piezoelectric transducer (PZT) is swept at 10 Hz and shifts the phase of the local oscillator (LO) relative to the squeezed light by several wavelengths. D1 and D2 are a matched pair of silicon photodiodes.

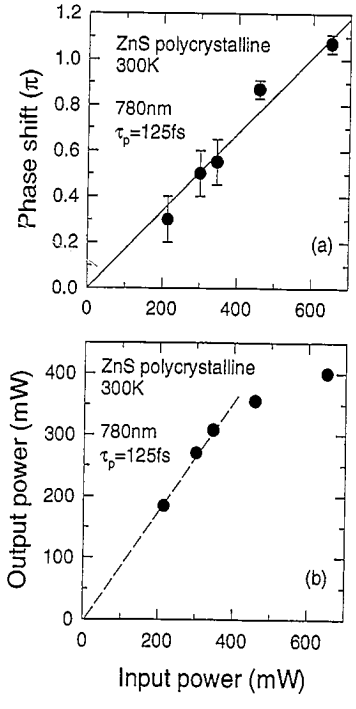

Fig. 2. (a) Maximum phase-shift determined by the fit of the spectra in Fig. 1. The slope of the linear fit through the data gives the nonlinear refractive index n_2. (b) Transmitted power as a function of the input power in the ZnS sample. The saturation above 300 mW is an indication of nonlinear multiphoton absorption processes that set in.

In the nonlinear regime careful positioning of the sample with respect to the focal plane of the two focusing lenses is critical in order to avoid phase front distortions that can decrease the contrast ratio of the interference at BS2. This point is illustrated in Fig. 4 where we show the intensity of the interference pattern with the sample purposely placed off focus for one of the lenses (Fig. 4a). The patterns where recorded by projecting the fringes at BS2 onto a screen and then scanning across the centre of the fringe pattern with a camera. The Sagnac was optimised at low power and the corresponding fringe pattern is reported in Fig. 4b. Increasing the power by a factor of 4, the nonlinear phase shift experienced by the two counter propagating pulses through

the sample is not the same and the corresponding relative phase shift ($\Delta\phi_1 - \Delta\phi_2 \sim \pi/2$) causes the central dark disk to be replaced by a bright fringe (Fig. 4c). A careful alignment of the Sagnac is thus necessary in order the detect squeezing. However, due to the departures of the beam splitting ratio from 50:50 over the beam width and laser bandwidth, even in optimum conditions the measured contrast ratio of the interferometer is about 70 and some

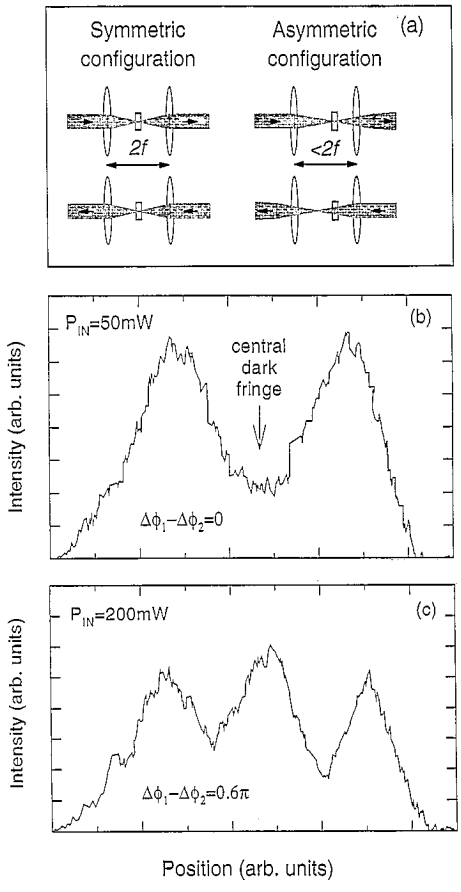

Fig. 4. Effect of the different phase shift experienced by the two counter-propagating pulses in a asymmetrically configured nonlinear interferometer. (a) Schematic diagram of the symmetric (lens separation = $2f$ and sample at the focussing point) and asymmetric (lens separation < $2f$ and the sample at the focus of only one of the two lenses) configuration. (b) Intensity of the interference fringe pattern at BS2 in the low power (linear) regime. (c) The same as (b) but in the nonlinear regime. The central bright fringe replacing the dark one in (b) arises because the two beams experience different self-phase modulation phase shifts. In this particular case the relative difference between $\Delta\phi_1 - \Delta\phi_2$ is $\sim \pi/2$.

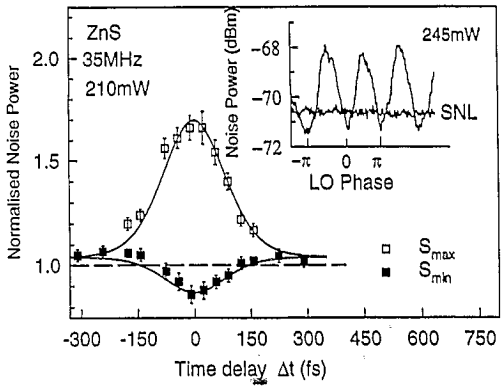

Fig. 5. Dependence of the maxima (open squares) and minima (black squares) of the phase dependent noise on the time delay Δt at 210 mW incident power. The solid lines are autocorrelations of a 125 fs pulse. The frequency was 35 MHz with a 3 MHz resolution bandwidth, and 300 Hz video bandwidth. Inset: phase dependent noise and shot noise level (SNL) measured with 245 mW in each beam of the Sagnac.

coherent "bright" squeezed light propagates along with the squeezed "vacuum".

The squeezed light was measured with a balanced homodyne detector scheme [10,11]. The local oscillator (LO) reference signal was obtained by splitting off 15% of the transmitted "bright" beam at BS1 and then overlapped again with the squeezed "vacuum" at a second 50:50 beam splitter BS3. The temporal overlap between the two beams was controlled by a delay line on the LO optical path, while the relative phase was swept out by a piezo transducer (PZT). The output beams from BS3 were focused at a pair of matched photodiodes and the photocurrent difference amplified and recorded by a spectrum analyzer.

In Fig. 5 we present our main result. In the inset we show noise traces at 35 MHz as a function of the phase shift between the squeezed light and the LO. When the LO and squeezed pulses were adjusted to arrive simultaneously at BS3 ($\Delta t = 0$), a phase dependent noise of period π is observed. Under identical conditions without the sample no such modulation is found, precluding contributions from pump laser instability or diode nonlinearity. The shot noise level (SNL) is recorded by presenting the same optical power to each photodiode from solely the LO input. The minimum noise ($S_{\min}$) drops 0.9 dB (20%) below this SNL, while the maximum noise (S_{MAX}) is enhanced by 2 dB (60%).

In the main part of the figure we show that the phase dependent noise is only seen when the LO pulses arrive together with the squeezed pulses. The experimental points are the maxima and minima of the normalised phase dependent noise at 35 MHz while the solid lines are the suitably normalised autocorrelation traces of the laser pulse. If the LO and the squeezed "vacuum" are not temporally overlapped ($|\Delta t| \gg \tau_p$) the shot-noise limit is recovered.

Similar results have been obtained in ZnSe at 960 nm, but we failed to observe any squeezing at 890 nm ($\hbar\omega \sim 0.52 E_g^{ZnSe}$), presumably due to the strong two-photon absorption at that wavelength.

In conclusion, we have measured the real and imaginary part of the susceptibility in ZnS and ZnSe near half-bandgap. We found values of n_2 in close agreement with recent theoretical and experimental evaluations. Our results suggest that the use of fs laser pulses with high peak power to produce a strong nonlinear phase shift, and the choice of photon energy below midgap in order to reduce nonlinear absorption losses are critical factors in obtaining large values of the figure of merit. Once these conditions are fulfilled, *quadrature* squeezed light can be generated in semiconductors using relatively simple experimental setups. The results indicate that our method is quite generally applicable to semiconductors, and opens the way for squeezed light generation at a wide range of wavelengths for possible applications in high-resolution spectroscopy, quantum nondemolition experiments, quantum communications, and low-light-level microscopy [12,13].

References

[1] L.A. Wu, H.J. Kimbe, J.L. Hall and H. Wu, Phys. Rev. Lett. 57 (1987) 2520.
[2] J. Merzt, T. Debuisschert, A. Heidmann, C. Fabre and E. Giacobino, Opt. Lett. 16 (1991) 1234.
[3] A.M. Fox, B. Huttner, J.F. Ryan, M.A. Pate and J.E. Roberts, Phys. Rev. A 50 (1994) 4415.
[4] M. Sheik-Bahae, D.C. Hutchings, D.J. Hagan and E.W. van Stryland, IEEE J. Quantum Electron. 27 (1991) 1296.
[5] R.H. Stolen and C. Lin, Phys. Rev. A 17 (1978) 1448.
[6] T.D. Krauss and F.W. Wise, Appl. Phys. Lett. 65 (1994) 1739.
[7] A.M. Fox, J.J. Baumberg, M. Dabbicco, B. Huttner and J.F. Ryan, Phys. Rev. Lett. 74 (1995) 1728.
[8] M. Rosenbluh and R.M. Shelby, Phys. Rev. Lett. 66 (1991) 153; P.D. Drummond, R.M. Shelby, S.R. Friberg and Y. Yamamoto, Nature 365 (1993) 307.
[9] K. Bergman, H.A. Haus, E.P. Ippen and M. Shirasaki, Opt. Lett. 19 (1994) 290.
[10] R.E. Slusher, P. Grangier, A. LaPorta, B. Yurke, Phys. Rev. Lett. 59 (1987) 2566.
[11] B. Huttner, J.J. Baumberg, J.F. Ryan and S.M. Barnett, Opt. Commun. 90 (1992) 128.
[12] See special issue on: Quantum Noise Reduction in Optical Systems – Experiments, Eds. E. Giacobino and C. Fabre, Appl. Phys. B 55 (1992) 189–303.
[13] M.I. Kolobov and P. Kumar, Opt. Lett. 18 (1993) 849.